CO_2 as a Probe for Monitoring the Surface Defects on TiO_2(110)—Temperature-Programmed Desorption

Tracy L. Thompson, Oliver Diwald, and John T. Yates, Jr.*

Surface Science Center, Department of Chemistry, University of Pittsburgh, Pittsburgh, Pennsylvania 15260

Received: April 11, 2003; In Final Form: June 27, 2003

The adsorption and thermal desorption of CO_2 bound to both oxidized and reduced TiO_2(110) surfaces has been studied using temperature-programmed desorption. For the stoichiometric and fully oxidized surface, a single thermal desorption feature (E_d = 48.5 kJ/mol) is measured and attributed to CO_2 bound to regular fivefold coordinated Ti^{4+} atoms. For the fully reduced TiO_2(110) surface, CO_2 binds not only to regular sites, but also to oxygen vacancy sites (E_d = 54.0 kJ/mol), created by thermal annealing. The variation in the characteristic CO_2 desorption kinetics was measured as a function of the surface reduction temperature, and the systematic production of increasing levels of surface defects is observed in the temperature range of 600−1100 K. This investigation was complimented by a comparison of the characteristic CO_2 desorption features from a TiO_2(110) surface which was prepared by sputtering and direct annealing, without annealing in O_2 flux. It was found that after annealing to temperatures above 900 K, the CO_2 thermal desorption is very similar for surfaces prepared by the two methods, regardless of surface preparation.

I. Introduction

The interaction of carbon dioxide and the TiO_2(110) surface was studied as a method for the characterization of the degree of surface reduction by annealing in a vacuum. It has been well documented that oxygen vacancy sites, created by thermal annealing in a vacuum, are the active sites for oxygen adsorption.[1] The use of a variety of techniques including ion scattering spectroscopy,[2] O_2 photodesorption,[3,4] and STM[5] have confirmed the presence of O vacancy sites after thermal annealing. The density of these vacancy sites can reach 8−10% of a single monolayer.[2−5] The nature of defects on TiO_2 is well explained in a recent review by Diebold.[6] Because the presence of these defect sites on TiO_2 is critical to its activity as a photooxidation catalyst, experimental methods that can be used to quantify the defect sites give insight into the overall activity of the single-crystal TiO_2 substrate. Previous work of this nature involves the interaction of various adsorbed species with both fivefold coordinated Ti^{4+} and oxygen vacancy sites (Ti^{3+}) as reported by Lu et al.[7] In that work, the adsorption of D_2O, $^{13}CH_2O$, and ^{15}NO and the subsequent thermal desorption of reduced products was studied as a function of the crystal annealing temperature. Results show a direct correlation between the surface annealing temperature and the yield of the reduced products. The onset temperature for O-vacancy defect formation, as measured in this manner, was 500 K.

Specific results relating to the nature of CO_2 chemisorption on TiO_2 have been obtained using both theoretical calculations for single crystals[8] and experimental measurements for both powdered[9−13] and single-crystal substrates.[14,15] For TiO_2(110), interactions of water and carbon dioxide were reported by Henderson.[14] In that work, it was shown that CO_2 binds to regular Ti^{4+} sites, as well as to oxygen vacancy sites, producing two features in the CO_2 thermal desorption spectra. The work to be presented here deals with the thermal desorption of CO_2 from TiO_2(110) where varying degrees of surface reduction affect the CO_2 thermal desorption behavior. Preparation procedure A involves heating the sputter-cleaned crystal to 900 K for 60 min in O_2 flux (5×10^{14} molecules/cm^2 s) and then cooling in O_2 flux. This crystal was then heated prior to each thermal desorption experiment to various temperatures ranging from 600 to 1100 K in a vacuum to produce different surface and bulk defect levels. Procedure A has been shown to oxidize Ti^{3+} interstitial species, creating regrown surface islands of fully oxidized $Ti^{4+}O_2$ in a (1 × 1) structure.[6,16,17] The area of the regrown islands increases with increasing annealing temperature in O_2, as shown in Stone et al.[16] In our procedure A, we believe the surface to consist of regular (1 × 1) islands where the irregularities created by sputtering are significantly smoothened.[17]

Also, comparative studies were done by using CO_2 as a probe for the defect density on a TiO_2(110) crystal which has been prepared via preparation procedure B, the so-called "bulk oxidation" technique,[18] which does not involve a full oxidation procedure in a controlled O_2 flux. In procedure B, the sputter-cleaned crystal was annealed in a vacuum to various temperatures ranging from 750 to 1100 K. No oxidation in O_2 flux was performed.

II. Experimental

The experiments reported here were done in an ultrahigh vacuum chamber with a base pressure below 1×10^{-10} mbar. The system is specially equipped with a differentially pumped quadrupole mass spectrometer (QMS) containing a small aperture of 1.6-mm diameter located 1 mm from the front surface of the TiO_2(110) crystal. This arrangement is ideal for temperature-programmed desorption (TPD) measurements which sample the front surface of the crystal. More specifications for the chamber used in these studies can be found in ref 19.

Crystals used for this investigation were obtained from Princeton Scientific Corporation with dimensions of 10 mm × 10 mm × 1 mm, with precut slots around all four edges to directly mount the crystal on a Ta support plate using Ta foil clips. The mounting of the crystal is done in such a way that

* Address correspondence to this author.

10.1021/jp030430m CCC: $25.00
Published on Web 09/25/2003

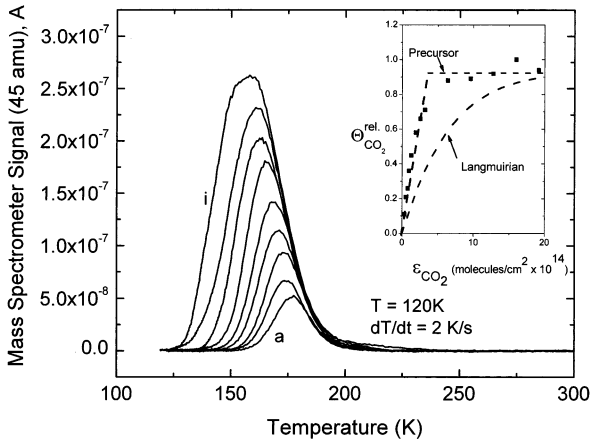

Figure 1. Coverage dependent thermal desorption spectra for $^{13}CO_2$ adsorbed on a fully oxidized TiO_2(110) surface. CO_2 exposures are (a) 3.5×10^{13} CO_2/cm^2; (b) 5.0×10^{13} CO_2/cm^2; (c) 8.0×10^{13} CO_2/cm^2; (d) 9.6×10^{13} CO_2/cm^2; (e) 1.3×10^{14} CO_2/cm^2; (f) 1.6×10^{14} CO_2/cm^2; (g) 2×10^{14} CO_2/cm^2; (h) 2.5×10^{14} CO_2/cm^2; (i) 3.5×10^{14} CO_2/cm^2.

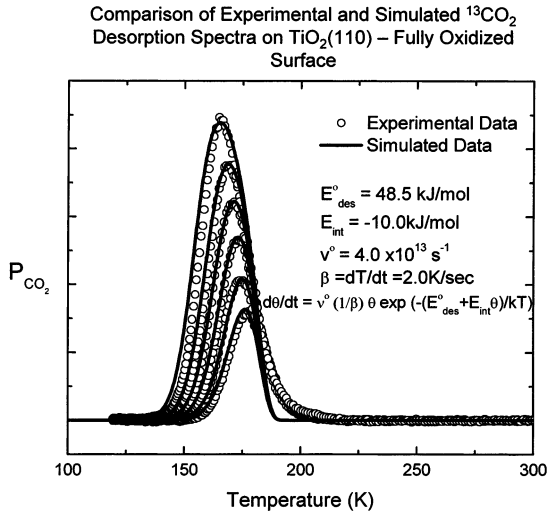

Figure 2. Simulated data versus experimental data for CO_2 thermal desorption from a fully oxidized TiO_2(110) surface for low coverages ranging from 1.5×10^{13} molecules/cm^2 to 1.5×10^{14} molecules/cm^2.

only the face of the crystal is exposed to the QMS during TPD measurements, or during dosing with the calibrated molecular beam doser. Resistive heating is done by passing current through two tungsten wires (0.38-mm diam) that are directly spot welded to the back of the Ta plate. Mounting in this manner allows for sample cooling to temperatures of 110 K and heating to 1100 K. Prior to experiments, the crystal is cleaned by successive intervals of Ar^+ sputtering (1500 V) and annealing to 900 K, until no traces of impurities were measured using AES. In preparation procedure A, the fully oxidized surface is obtained by further annealing the crystal to temperatures of 900 K in O_2 flux of 5×10^{14} molecules/cm^2 s for 1 h. The crystal is also cooled in the same flux of O_2(g). Reduction of the crystal was done by annealing in vacuum to various temperatures each for 1 h, starting at 600 K. In preparation procedure B, the clean crystal surface was sputtered (500 eV, 15 min) and then annealed in vacuum to temperatures in the range of 750−1100 K. For the CO_2 thermal desorption measurements shown here, a heating rate of 2 K/s was used.

$^{13}CO_2$ (Cambridge Isotope Laboratories, 99%) was used in these experiments. All gas exposures were carried out using a calibrated microcapillary array beam doser (7.3×10^{13} CO_2 molecules/Torr cm^2 s) at a crystal temperature of 110 K.[20] After gas exposure, the sample was then rotated into position directly in front of the QMS aperture.

III. Results

A. Thermal Desorption of CO_2 from TiO_2. Figure 1 shows thermal desorption spectra of varying $^{13}CO_2$ exposures for a fully oxidized TiO_2(110) surface. For this surface, low exposures of CO_2 reveal a single desorption peak at approximately 170 K, which grows to saturation at exposures of approximately 3×10^{14} molecules/cm^2. The inset of Figure 1 shows the asymptotic rise of the $^{13}CO_2$ coverage to near saturation as the exposure is increased. The CO_2 feature seen at low coverages at about 170 K is attributed to CO_2 molecules that are bound to regular five-coordinate Ti^{4+} sites. The first-order thermal desorption spectra for the oxidized surface was simulated for CO_2 coverages between 1.5×10^{13} molecules/cm^2 and 1.5×10^{14} molecules/cm^2 according to the Polanyi−Wigner equation:

$$-\frac{dN}{dT} = R_{des} = \upsilon^0 \cdot \frac{1}{\beta} N \exp\left[-\frac{(E^{\circ}_{des} + E_{int}N)}{kT}\right] \qquad (1)$$

where R_{des} is the rate of desorption, dN/dt, N is the coverage, υ° is the preexponential factor, $\beta = dT/dt$, E°_{des} is the zero-coverage desorption activation energy, and E_{int} is the energy of the lateral interactions between adsorbed CO_2 molecules. Figure 2 shows both the simulated data as well as the experimental results. It was found that CO_2, bound to regular fivefold coordinated Ti^{4+} sites, exhibits a desorption activation energy of $E^{\circ}_{des} = 48.5$ kJ/mol, with a preexponential term of 4×10^{13} s^{-1} and an interaction energy of −10 kJ/mol, signifying repulsive interactions between adsorbates. The linear increase in $^{13}CO_2$ coverage during the majority of the adsorption process indicates that adsorption occurs via a mobile precursor mechanism.[21] The fitting procedure has favored the leading edge of the desorption pulse since errors due to defect sites can easily influence the trailing edge.

Upon annealing the crystal in vacuum to higher temperatures, the appearance of an additional $^{13}CO_2$ peak desorbing at higher temperatures in the TPD spectra is evident, as shown in Figure 3 where a full set of coverage dependent TPD spectra is shown for each reduction temperature in the range of 600−1100 K. Because of small experimental variations from day to day for the different adsorption measurements, a through *f*, we have chosen to normalize all of the $^{13}CO_2$ desorption spectra to the maximum coverage in each presentation. The appearance of the high-temperature TPD feature (at about 200 K) as a shoulder to the peak attributed to CO_2 bound to regular sites is first seen clearly on the surface that has been prepared by annealing at 700 K for 1 h. Because this peak grows after annealing to higher temperatures, it is attributed to CO_2 bound to the defective TiO_2 surface, specifically to oxygen vacancy sites. The development of the spectra for various annealing temperatures indicates that a maximum number of defects are achieved after annealing in vacuum to temperatures of ∼900 K.

A simulation using the same method as for the data shown in Figure 2 was done for the high-temperature CO_2 desorption feature, also for low coverages of CO_2 (1.5×10^{13} CO_2/cm^2 to 1.5×10^{14} CO_2/cm^2) as shown in Figure 4. Isolation of the high-temperature feature was achieved by subtraction of the low-temperature CO_2 desorption feature from a fully oxidized surface from the data presented in Figure 3d. The preexponential term was set to 4×10^{13} s^{-1} and the resulting desorption activation energy was $E^{\circ}_{d} = 54.0$ kJ/mol. Again, kinetic fits to the leading edge were favored in the analysis. The calculated value for the

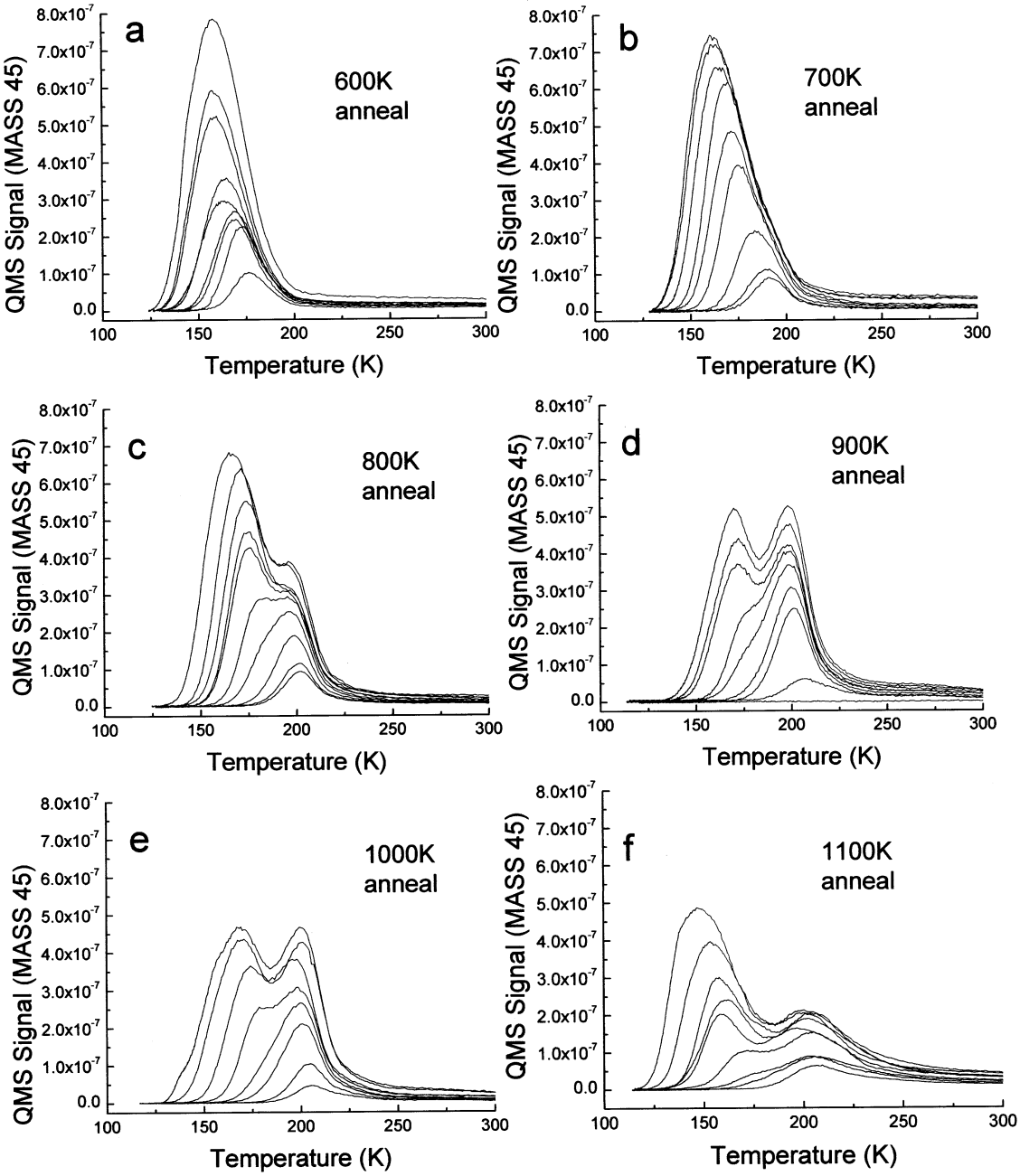

Figure 3. Normalized coverage dependent thermal desorption spectra for $^{13}CO_2$ adsorbed on TiO_2(110) for surfaces preannealed to (a) 600 K, (b) 700 K, (c) 800 K, (d) 900 K, (e) 1000 K, (f) 1100 K. In these experiments, the $^{13}CO_2$ exposure ranged from 1.5×10^{13} molecules/cm^2 to 3.5×10^{14} molecules/cm^2.

repulsive interaction energy between adsorbed CO_2 molecules at Ti^{3+} sites was estimated as -7 kJ/mol.

B. CO_2 Thermal Desorption Spectra from a Sputtered and Annealed Surface. For the crystal surface which has been prepared via the "bulk assisted" oxidation technique,[18] (procedure B), CO_2 thermal desorption spectra are shown as a function of the annealing temperature in Figure 5. The CO_2(g) exposure is the same for each experiment in this case. For lower annealing temperatures (750 K), a very broad single desorption feature is measured spanning a temperature range from ~140 K to 220 K. With increasing annealing temperature, this broad feature becomes sharper, and after annealing to temperatures above 900 K, a two-peak thermal desorption is observed, qualitatively similar to that seen in Figure 3c−f.

IV. Discussion: Thermal Desorption of CO_2 from TiO_2(110)

Anion vacancy defect sites are important in the application of TiO_2 to photooxidation chemistry, since O_2 reactant is preferentially adsorbed on these sites.[1] Previous studies have measured the presence of these sites using chemical reduction reactions which are specific for these sites.[3] However, a more simple method which is sensitive to the defect sites would be useful, and the specific high binding energy adsorption behavior of CO_2 on defect sites serves this purpose. Henderson has observed the characteristic two-step desorption process which is indicative of the presence of both vacancy defect and nondefective TiO_2 sites.[14] Our experiments agree qualitatively with this work, and we have measured the activation energy

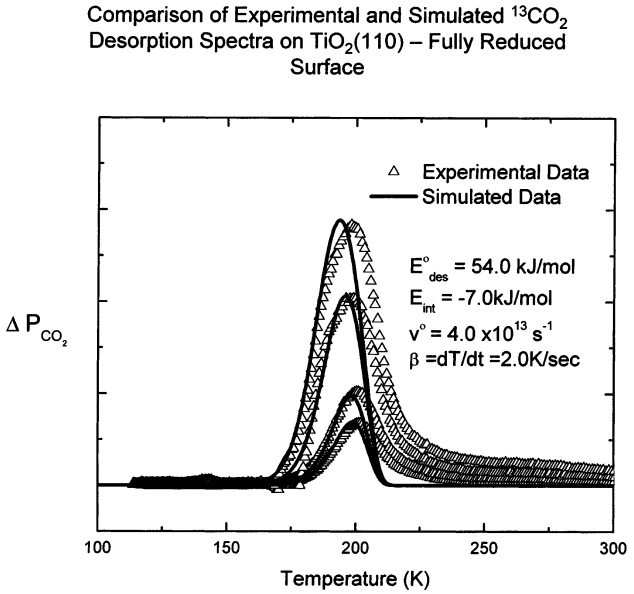

Figure 4. Simulated data versus experimental data for CO_2 thermal desorption from a fully reduced (900 K) TiO_2(110) surface for low coverages, ranging from 1.5×10^{13} molecules/cm^2 to 1.5×10^{14} molecules/cm^2.

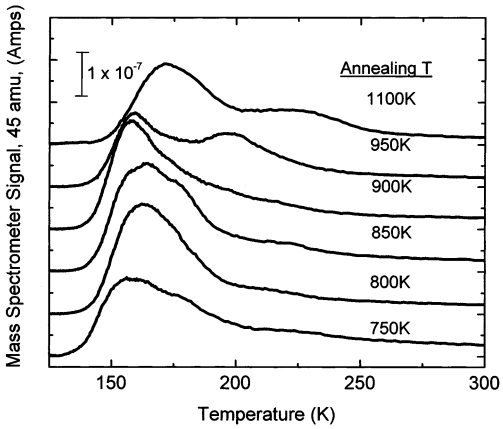

Figure 5. Characteristic CO_2 thermal desorption spectra from a TiO_2(110) crystal that has been sputtered then annealed prior to CO_2 adsorption according to procedure B. Spectra are shown for various preannealing temperatures, as noted. Each spectrum shown is for the same CO_2 exposure, 1.5×10^{14} CO_2/cm^2.

for desorption of the two types of CO_2. We find that under the adsorption temperature conditions of our experiment it is difficult to completely saturate the CO_2 species which forms on the nondefective surface sites, so the ratio of the population of the two desorption states cannot be used to determine the ratio of the sites.

For CO_2 on TiO_2(110) and on partially reduced TiO_2(110) (adsorption kinetic experiments not shown on the latter surface), adsorption occurs via a mobile precursor mechanism causing a linear uptake curve to be observed as shown, for example, in the inset to Figure 1. This observation implies that delivery of the adsorbate to the higher binding energy defect sites occurs by means of a weakly held species which can sample multiple sites before adsorption.[21] CO_2 adsorption via a Langmuirian kinetic model is not appropriate as seen in the inset to Figure 1.

For CO_2 adsorption on the fully oxidized surface, where the CO_2 is bound to Ti^{4+} sites, we measure a zero-coverage activation energy for CO_2 desorption of 48.5 kJ/mol. Repulsive lateral interactions (~10 kJ/mol) occur between these species. Theoretical calculations report that the binding energy of CO_2 to TiO_2(110) occurs with an energy of 65 kJ/mol, in approximate agreement with our measurement of 48.5 kJ/mol.[8] Calculations indicate that repulsive energies of about −15 kJ/mol would be expected for CO_2 on TiO_2(110)[8] in satisfactory agreement with our measurements.

From the comparison of the experiment and the simulations of the kinetic behavior for CO_2 desorption from the defect sites produced by annealing TiO_2(110) in vacuum above about 700 K, we measure a zero-coverage activation energy of ~54 kJ/mol. It is surprising that this energy is only about 6 kJ/mol above the activation energy for desorption from the fully oxidized surface, since the electronic character of the defect site (Ti^{3+}) is very different from the Ti^{4+} site on the oxidized surface. The repulsive $CO_2 \cdots CO_2$ interaction energy for CO_2 on the defect sites is somewhat less than for CO_2 on the oxidized surface, possibly because of the greater spatial separation of defect sites.

The sequence of CO_2 thermal desorption spectra seen in Figure 3 fit together into a logical sequence up to an annealing temperature of 1000 K. The high temperature desorption process becomes systematically more prominent for increasing annealing temperatures. However, annealing at 1100 K leads to a change in the nature of the sequence, with the development of a more prominent lower temperature CO_2 desorption state. The 1100 K temperature is the onset temperature for a massive reconstruction of TiO_2(110)−(1 × 1) to produce the (2 × 1) surface phase for which STM structural studies and models for this structure have been presented.[16,22−24]

Apparently, the thermal treatment of TiO_2(110) surfaces made by preparation method A and method B yield similar CO_2 desorption behavior when high-temperature annealing occurs into the temperature range where the (1 × 1) to (2 × 1) reconstruction occurs, as seen from comparison of Figure 3f and the upper CO_2 desorption spectrum in Figure 5.

V. Conclusions

The thermal desorption characteristics for CO_2 from TiO_2(110) have been studied. The effect of surface preparation on these experiments has also been investigated. The following conclusions can be drawn:

(1) Two types of adsorption sites, assigned as nondefective and defective, are available for the adsorption of CO_2 on a TiO_2(110) vacuum annealed surface. The thermal desorption of CO_2 from TiO_2(110) can therefore be used as a tool to investigate defect production on TiO_2(110) surfaces.

(2) For a TiO_2(110) surface which has been prepared by Ar^+ sputtering and subsequent annealing, the characteristic CO_2 thermal desorption becomes more like that of a fully oxidized (and then reduced crystal) with increasing annealing temperature.

Acknowledgment. This work was supported by the DoD Multidisciplinary University Research Initiative (MURI) program administered by the Army Research Office under Grant DAAD-19-01-0-0619. O. Diwald gratefully acknowledges the support by the Austrian Science Fund (Project J 2058). We would like to thank Mr. Tykhon Zubkov for helpful advice and direction. We also thank an anonymous reviewer for finding an error in our experimental measurements and advising us privately of this error.

References and Notes

(1) Henderson, M. A.; Epling, W.; Perkins, C.; Peden, C.; Diebold, U. *J. Phys. Chem. B* **1999**, *103*, 5328−5337.

(2) Pan, J. M.; Maschhoff, B. L.; Diebold, U.; Madey, T. E. *J. Vac. Sci. Technol., A* **1992**, *10*, 2470−2476.

(3) Lu, G.; Linsebigler, A.; Yates, J. T., Jr. *J. Chem. Phys.* **1995**, *102*, 4657−4662.
(4) Rusu, C. N.; Yates, J. T., Jr. *Langmuir* **1997**, *13*, 4311−4316.
(5) Diebold, U.; Lehman, J.; Mahmoud, T.; Kuhn, M.; Leonardello, G.; Hebenstreit, W.; Schmid, M.; Varga, P. *Surf. Sci.* **1998**, *411*, 137−153.
(6) Diebold, U. *Surf. Sci. Rep.* **2003**, *48*, 53−229.
(7) Lu, G.; Linsebigler, A.; Yates, J. T., Jr. *J. Phys. Chem.* **1994**, *98*, 11733−11738.
(8) Markovits, A.; Fahmi, A.; Minot, C. *THEOCHEM* **1996**, *371*, 219−235.
(9) Tanaka, K.; White, J. M. *J. Phys. Chem.* **1982**, *86*, 3977−3980.
(10) Tanaka, K.; Miyahara, K.; Toyoshima, I. *J. Phys. Chem.* **1984**, *88*, 3504−3508.
(11) Yanagisawa, Y.; Sumimoto, T. *Appl. Phys. Lett.* **1994**, *64*, 3343−3344.
(12) Yanagisawa, Y. *Energy Concers. Mgmt.* **1995**, *36*, 443−446.
(13) Liao, L. F.; Lien, C. F.; Shieh, D. L.; Chen, M. T.; Lin, J. L. *J. Phys. Chem. B* **2002**, *106*, 11240−11245.
(14) Henderson, M. A. *Surf. Sci.* **1998**, *400*, 203−219.
(15) Göpel, W.; Rocker, G.; Feierabend, R. *Phys. Rev. B* **1983**, *28*, 3427−3438.
(16) Stone, P.; Bennett, R. A.; Bowker, M. *New J. Phys.* **1999**, *1*, 1.1−1.12.
(17) Li, M.; Hebenstreit, W.; Gross, L.; Diebold, U.; Henderson, M. A.; Jennison, D. R.; Schultz, P. A.; Sears, M. P. *Surf. Sci.* **1999**, *437*, 173−190.
(18) Henderson, M. A. *Surf. Sci.* **1999**, *419*, 174−187.
(19) Hanley, L.; Guo, X.; Yates, J. T., Jr. *J. Chem. Phys.* **1989**, *91*, 7220−7227.
(20) Yates, J. T., Jr. *Experimental Innovations in Surface Science*; AIP and Springer-Verlag: New York, 1998; p 604.
(21) Weinberg, W. H. In *Kinetics of Interface Reactions*; Grunze, M., Kreuzer, H. J., Eds.; Springer-Verlag: New York, 1987; p 95.
(22) Tanner, R. E.; Castell, M. R.; Briggs, G. A. D. *Surf. Sci.* **1998**, *412/413*, 672−681.
(23) Pang, C. L.; Haycock, S. A.; Raza, H.; Murray, P. W.; Thornton, G.; Gulseren, O.; James, R.; Bullet, D. W. *Phys. Rev. B* **1998**, *58*, 1586−1589.
(24) Diebold, U.; Anderson, J. F.; Ng, K. O.; Vanderbilt, D. *Phys. Rev. Lett.* **1996**, *77*, 1322−1325.